

# A random matrix model with two localization transitions.

V. E. Kravtsov,<sup>1,2</sup> I. M. Khaymovich,<sup>3,4,\*</sup> E. Cuevas,<sup>5</sup> and M. Amini<sup>6</sup>

<sup>1</sup>*Abdus Salam International Center for Theoretical Physics, Strada Costiera 11, 34151 Trieste, Italy*

<sup>2</sup>*L. D. Landau Institute for Theoretical Physics, Chernogolovka, Russia*

<sup>3</sup>*Low Temperature Laboratory, Department of Applied Physics, Aalto University, FI-00076 Aalto, Finland*

<sup>4</sup>*Institute for Physics of Microstructures, Russian Academy of Sciences, 603950 Nizhny Novgorod, GSP-105, Russia*

<sup>5</sup>*Departamento de Física, Universidad de Murcia, E30071 Murcia, Spain*

<sup>6</sup>*Department of Physics, University of Isfahan(UI), Hezar Jerib, 81746-73441, Isfahan, Iran*

Motivated by the problem of Many-Body Localization and the recent numerical results for the level and eigenfunction statistics on the random regular graphs, a generalization of the Rosenzweig-Porter random matrix model is suggested that possesses two localization transitions as the parameter  $\gamma$  of the model varies from 0 to  $\infty$ . One of them is the Anderson transition from the localized to the extended states that happens at  $\gamma = 2$ . The other one at  $\gamma = 1$  is the transition from the extended non-ergodic (multifractal) states to the extended ergodic states similar to the eigenstates of the Gaussian Orthogonal Ensemble. We computed the two-level spectral correlation function, the spectrum of multifractality  $f(\alpha)$  and the wave function overlap which all show the transitions at  $\gamma = 1$  and  $\gamma = 2$ .

*Introduction*— Motivated by the problem of Many-Body (MB) Localization [1] and applicability of the Boltzmann's energy equipartition hypothesis in interacting disordered media [2], there was recently a revival of interest to the Anderson localization (AL) problem on hierarchical lattices such as the Bethe lattice (BL) or the random regular graph (RRG). Due to hierarchical structure of the Fock space connected by the two-body interaction, existence of the non-ergodic extended phase on disordered hierarchical lattices would imply a breakdown of conventional Boltzmann statistics in interacting MB systems and emergence of a phase of a “bad metal” with rather exotic properties. However, even for the single-body problem existence of such a phase in a finite interval of disorder strengths is a highly non-trivial issue.

According to earlier studies [3, 4] there is only one transition in such models at  $W = W_{AT}$  which is the AL transition that separates the localized and ergodic extended states. However, recent numerical studies [5] of level statistics on RRG seem to indicate on the second transition at  $W = W_{ET} < W_{AT}$  which is identified as the transition between the ergodic and non-ergodic extended states. Subsequent studies [6, 7] raise doubts about the existence of the second transition on RRG. Numerical results of Ref. [6] indicate on the non-ergodic states on RRG in a wide range of disorder strengths down to very low disorder  $W = 5 \ll W_{AT} \approx 17.5$ , while in Ref. [7] it is demonstrated how an apparent non-ergodic behavior for the intermediate matrix sizes  $N$  in Levy Random Matrix (RM) ensemble evolves into the ergodic one at larger  $N$ 's.

Complexity of RRG and the controversy associated with existence of the *ergodic* transition at  $W = W_{ET}$  necessitate a search for a simpler RM model in which such a transition may occur. An important heuristic argument to construct such a model is that RRG with on-site energy disorder is essentially a two-step disorder ensemble. The disorder of the first level is the structural disorder

due to the random structure of RRG where each of  $N$  sites of the graph is connected with the fixed number  $K+1$  of other sites in a random manner. An ensemble of such tight-binding models with the hopping integral between the connected sites equal to -1 and all on-sites energies equal to 0 is believed to be equivalent to the ensemble of Gaussian RMs [8]. The disorder of the second level is produced by randomization of the on-site energies  $\varepsilon_i$  fluctuating independently around zero with the distribution function  $p(\varepsilon)$ . For numerical calculations this distribution is often taken in the form  $p(\varepsilon) = W^{-1} \theta(W/2 - |\varepsilon|)$ , with  $\theta(x)$  being the Heaviside step function.

One can expect that the following RM ensemble (the Rosenzweig-Porter (RP) ensemble) is a close relative of RRG with on-site energy disorder. It is an ensemble of  $N \times N$  random Hermitian matrices which entries  $H_{nm}$  with  $n > m$  are independent random Gaussian real numbers fluctuating around zero with the variance  $\langle H_{nm}^2 \rangle = \sigma/2$ , while the diagonal elements have the same properties with the variance  $\langle H_{nn}^2 \rangle = 1$ . The case  $\sigma = 1$  corresponds to the Gaussian Orthogonal Ensemble (GOE) and represents the structural disorder in RRG, while the additional on-site energy disorder in RRG corresponds to  $\sigma < 1$ . One can estimate the strength of disorder required for the AL transition as corresponding to the typical fluctuation of diagonal matrix element equal to the typical off-diagonal matrix element times the coordination number  $K+1$ . For the coordination number  $K \sim N$  (each site is connected with any other one) this results in  $\sqrt{\sigma}N \sim 1$ , or  $\sigma \sim 1/N^2$ . However, this estimation does not take into account a random, sign-alternating character of the off-diagonal matrix elements. It is likely that for sign-alternating hopping there is another relevant effective coordination number  $\sim \sqrt{N}$  resulting in the critical scaling  $\sigma \sim 1/N$ . As we show below it corresponds to the ergodic transition.

To address both cases we consider the model:

$$\langle H_{nn}^2 \rangle = 1, \quad \langle |H_{n \neq m}|^2 \rangle = (\beta/2) \sigma = \lambda^2/N^\gamma, \quad (1)$$

where  $\lambda$  is a (redundant) number of order  $O(N^0)$ , and  $\beta = 1$  or  $2$  stand for the orthogonal (ORP) or unitary (URP) Rosenzweig-Porter models. The URP model has been considered long ago [9] and the conclusion was that the AL transition happens at  $\gamma = 2$  where the spectral form-factor (two-level correlation function) is neither of the Wigner-Dyson nor of the Poisson form.

In this Letter we show that the above model contains not one but two transitions. One of them happens indeed at  $\gamma = 2$  and corresponds to the transition from the extended to the localized states. However, the extended states emerging at  $\gamma < 2$  are not ergodic: their support set contains infinitely many  $N^{D_1}$  sites in the  $N \rightarrow \infty$

limit, which, however, is a zero fraction of all sites, since  $D_1 < 1$ . Such non-ergodic extended states on RRG are recently discussed in Ref. [6]. With further decrease of  $\gamma$  the second transition at  $\gamma = 1$  happens which is a transition from the non-ergodic to the ergodic extended states with  $D_1 = 1$  similar to the eigenstates of the GOE. In contrast to RRG we demonstrate the existence of the second transition by rigorous calculation of the level statistics which is a proper generalization of Ref. [9] as well as by simple perturbative arguments supported by the extensive numerical calculations.

*Spectral form-factor.*—We start by Eq. (3.2) of Ref. [9] for the spectral form-factor  $C(t, t') = \sum_{n \neq m} e^{itE_m + it'E_n}$  ( $\{E_n\}$  is a set of eigenvalues of  $H$ ) which was derived for URP model Eq. (1) using the Itzikson-Zuber formula of integration over unitary group.

$$C(t, t') = \frac{e^{-\sigma(t^2+t'^2)/2}}{N\tau\tau'} \oint_{\Gamma_R} \frac{dz}{2\pi i} \oint_{\Gamma_R} \frac{dz'}{2\pi i} e^{i(tz+t'z')} \left[ g(z, z')^N \left( 1 + \frac{\tau\tau'}{(z' - z - \tau)(z' - z + \tau')} \right) - \rho(z)^N \rho(z')^N \right], \quad (2)$$

In this exact formula integration is extended over the contour  $\Gamma_R$  that encompasses the real axis and  $\tau = it\sigma$ . The functions  $g(z, z')$  and  $\rho(z) = 1 + \tau\alpha(z)$  depend on the diagonal disorder distribution  $p(a)$  through  $\alpha(z) = \int p(a)da/(z - a) = \langle (z - a)^{-1} \rangle$  and are defined as follows:

$$g(z, z') = 1 + \tau\alpha(z) + \tau'\alpha(z') - \frac{\tau\tau'}{z - z'} [\alpha(z) - \alpha(z')]. \quad (3)$$

In order to do the limit of infinite matrix size  $N \rightarrow \infty$  we make a re-scaling:

$$(t, t') = \frac{T}{2} \pm N^{\Delta_t} s \quad (4)$$

$$(z, z') = x \pm \frac{y}{2N^{\Delta_z}} - \frac{i\delta}{N^{\Delta_z}} (q, q'), \quad (5)$$

where  $q, q' = \pm 1$  for the part of the contour below and above the real axis. The exponents  $\Delta_t > 0$  and  $\Delta_z > 0$  should be chosen so that (i) finite limits  $\lim_{N \rightarrow \infty} [g(z, z')]^N$  and  $\lim_{N \rightarrow \infty} [\rho(z)]^N$  exist, and (ii) the entire expression  $C(t, t')$  is finite in the  $N \rightarrow \infty$  limit. One can show that the choice

$$\Delta_t = \gamma - 1, \quad \Delta_z = 1, \quad (6)$$

satisfies all these conditions if  $\gamma > 1$ . Now doing the limit  $N \rightarrow \infty$  at fixed  $T, s, x, y$  we observe that the parameter  $\gamma$  enters the limiting expression Eq. (2) only in the exponents  $e^{-\sigma(t^2+t'^2)/2} \rightarrow e^{-\lambda^2 N^{\gamma-2} s^2}$  and  $e^{i(tz+t'z')} = e^{iTx+iN^{\gamma-2}sy}$ .

This observation immediately tells us that for  $\gamma > 2$  the spectral form-factor  $C(t, t')$  vanishes, which leads

to completely uncorrelated energy levels and the exact Poisson statistics. In the case  $\gamma = 2$  considered in Ref. [9] the level statistics is different from Poisson, as  $C(t, t') = 2\pi p(0)\delta(T)[R(s) - 1]$  is not zero. However, the level compressibility equals unity

$$\chi = R(0) = 1. \quad (7)$$

like for uncorrelated energy levels. Thus the negative correlation background in the density of states correlation function  $Y(r) = (2\pi)^{-1} \int_{-\infty}^{+\infty} R(s = u N p(0)) e^{-iur} du$  at small energy separations  $r = (E - E')/\delta$  ( $\delta = (N p(0))^{-1}$  is the mean level spacing) is compensated in the integral  $\int_{-\infty}^{+\infty} Y(r) dr = R(0)$  by the positive correlation background at larger  $r$ .

One can easily see that Eq. (7) remains valid also in the entire region  $1 < \gamma \leq 2$ , since at  $s = 0$  the  $\gamma$ -dependent exponents  $e^{-\lambda^2 N^{\gamma-2} s^2}$  and  $e^{iN^{\gamma-2}sy}$  are equal to 1 anyway. In Fig. 1 we plot the unfolded spectral form factor  $R(t = (t - t')\delta)$  for the two phases: (i) the critical phase of the AL transition at  $\gamma = 2$  and (ii) the intermediate phase at  $1 < \gamma < 2$ . The analytical formula for it is given in the Supplementary Material (SM) [10]. One can see that while at  $\gamma = 2$  the function  $R(t)$  has a non-trivial  $N \rightarrow \infty$  limit, for  $1 < \gamma < 2$  the limit coincides with that of the GUE, except for the point  $t = 0$  where there is a jump in  $R(t)$ . This jump is a hallmark of the intermediate phase. To demonstrate this more clearly we blow up the region of small  $t$  by re-scaling the variable  $t \Rightarrow u = (t - t')\delta N^{2-\gamma}$ . In this new variable  $S(u) = R(uN^{\gamma-2})$  has a non-GUE  $N \rightarrow \infty$  limit which is shown in the insert to Fig. 1. It

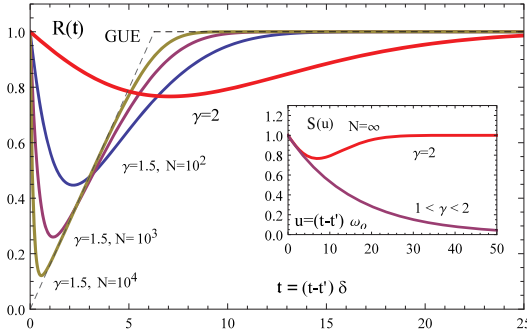


FIG. 1: (Color online) Unfolded spectral form-factor  $R(t = (t - t')\delta)$  ( $\delta = (p(0)N)^{-1}$  is the mean level spacing near the energy  $E = 0$ ) for the Rosenzweig-Porter model with  $\Lambda = \lambda p(0) = 0.1$  for two different phases: (i)  $\gamma = 2$  and (ii)  $1 < \gamma < 2$  for  $\gamma = 1.5$  and  $N = 10^2, 10^3, 10^4$ . The falling part corresponds to attraction of levels while the rising part corresponds to repulsion of levels. The GUE form-factor is shown by a dashed line. The Poisson distribution corresponds to  $R(t) = 1$ . In the insert: the spectral form-factor in the variable  $u = (t - t')\omega_o$  with  $\omega_o = N^{1-\gamma}/p(0)$  which has a non-GUE limit as  $N \rightarrow \infty$ . The GUE spectral form-factor in this variable is just zero in the limit  $N \rightarrow \infty$ .

is remarkable that the limiting  $S(u)$  correlation function does not depend on  $\gamma$  in the entire region  $1 < \gamma < 2$  and is given by a simple exponential:

$$S(u) = e^{-2\pi\Lambda^2 u}, \quad 1 < \gamma < 2. \quad (8)$$

Note that the method of re-scaling Eqs. (4, 5) fails for  $\gamma < 1$ . The physical reason for the failure is that the scale  $\omega_o = \delta N^{2-\gamma} = O[N^{1-\gamma}]$  which enters the dimensionless variable  $u = (t - t')\omega_o$ , for  $\gamma < 1$  grows with increasing  $N$  and exceeds the spectral band-width  $D \sim O(1)$ . As the energy difference  $\omega$  between the two states is bounded from above by  $D$ , the lower bound  $u_<$  of  $u$  where Eq. (8) holds, grows as  $N^{1-\gamma} \rightarrow \infty$ . For  $u < u_<$  the form-factor saturates at  $S(u_<) \rightarrow 0$ , so that the GOE limit  $S(u) = 0$  is reached. Thus  $\gamma = 1$  must be a second transition point such that for  $\gamma < 1$  the jump at  $t = 0$  in the  $N \rightarrow \infty$  limit of  $R(t)$  disappears, and it acquires a pure GUE form typical for the ergodic extended state.

*Multifractal eigenfunction statistics for  $1 < \gamma < 2$ .* Now let us consider the distribution of eigenfunction amplitudes  $P(x = N|\psi(r_o)|^2)$  in a certain observation point  $r_o$ . As the off-diagonal matrix elements are small, one can employ the perturbation theory. The first order perturbation theory gives for the amplitude:

$$|\psi_n(r_m)|^2 = \frac{|H_{nm}|^2}{(E_n - E_m)^2}, \quad (n \neq m) \quad (9)$$

where the maximum of  $\psi_n(r)$  is supposed to be at  $r = r_n$ .

Consider the regular part of the characteristic function  $Q(\xi) = \int_{-\infty}^{\infty} \langle \delta(x - N|\psi(r_o)|^2) \rangle e^{i\xi x} dx = \langle e^{i\xi N|\psi(r_o)|^2} \rangle$ .

For the Gaussian disorder distribution  $p(\varepsilon) = \frac{e^{-\varepsilon^2/2}}{\sqrt{2\pi}}$  and a real  $H_{nm} = V$  we obtain  $Q(\xi) = \mathcal{Q}(\xi N\sigma)$ , where:

$$\mathcal{Q}(\zeta) = e^{-i\zeta/2} \operatorname{Erfc} \left( \sqrt{\frac{-i\zeta}{2}} \right) \approx 1 - \sqrt{\frac{-2i\zeta}{\pi}}. \quad (10)$$

The function  $P(x) = \int_{-\infty}^{\infty} e^{-i\zeta \frac{x}{N\sigma}} \mathcal{Q}(\zeta) \frac{d\zeta}{2\pi N\sigma}$  at  $x \gg N\sigma \sim O(N^{1-\gamma})$  is dominated at  $\gamma > 1$  by small  $\zeta \ll 1$ . That is why it is only the expansion of Eq. (10) at small  $\zeta$  what matters for  $P(x)$  at  $\gamma > 1$ . Thus we obtain for the regular part of the eigenfunction distribution  $P(x)$ :

$$P(x) = \frac{1}{\sqrt{2\pi}} \frac{(N\sigma)^{1/2}}{x^{3/2}}. \quad (11)$$

There are two normalization conditions for  $P(x)$ : the normalization of probability Eq. (12) and the normalization of the wave function Eq. (13):

$$\int_0^{\infty} P(x) dx = 1, \quad (12)$$

$$\int_0^{\infty} x P(x) dx = 1. \quad (13)$$

Eq. (12) imposes a cut-off  $x_{\min} \sim N^{-(\gamma-1)}$  to Eq. (11) at small  $x$ , while Eq. (13) determines the upper cut-off  $x_{\max} \sim N^{\gamma-1}$ . A caution, however, should be taken: by normalization  $\sum_i |\psi(i)|^2 = 1$  the amplitude  $|\psi(r_o)|^2 \leq 1$  on any lattice site cannot exceed 1, and therefore  $x \leq N$ . One can see that the above estimation for  $x_{\max}$  is valid only for  $\gamma < 2$  when  $N^{\gamma-1} \ll N$ . For  $\gamma > 2$  a correct  $x_{\max} = N$ . In order to compensate for the deficiency of normalization in Eq. (13) one has to assume a *singular* part of  $P(x) = \mathcal{P}(x) + A \delta(x - N)$ . One can see that for  $\gamma > 2$  Eq. (13) is dominated by the singular term, and  $A = N^{-1}$ . This corresponds to the strongly localized wave functions. The mechanism of emergence of the singular term at the AL transition at  $\gamma = 2$  is somewhat similar to the Bose-condensation, where the singular term also appears because of the deficiency of normalization of the Bose-Einstein distribution.

Now consider the region  $1 < \gamma < 2$ . One can express the distribution function Eq. (11) through the *spectrum of fractal dimensions* [6, 11]:

$$f(\alpha) = \lim_{N \rightarrow \infty} \ln[xN\mathcal{P}(x)]/\ln N, \quad \alpha = 1 - \ln x/\ln N. \quad (14)$$

So we obtain for  $1 < \gamma < 2$  (see Fig. 2(c)):

$$f(\alpha) = \frac{\alpha}{2} + 1 - \frac{\gamma}{2}, \quad (2 - \gamma = \alpha_{\min} < \alpha < \alpha_{\max} = \gamma). \quad (15)$$

At the AL transition point  $\gamma = 2$  the function  $f(\alpha)$  has the same triangular shape as at  $W = W_{AT}$  on RRG. It is remarkable that in the entire region  $1 \leq \gamma \leq 2$  the symmetry [11, 12]  $f(1+x) = f(1-x) + x$  holds.

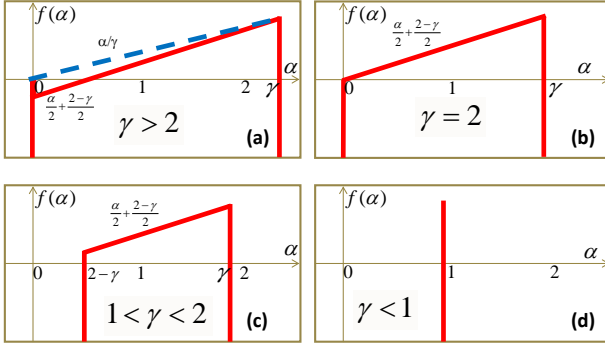


FIG. 2: (Color online) The spectrum of fractal dimensions: (a) the singular spectrum in the localized phase at  $\gamma > 2$ . It corresponds to the same exponent  $\tau(q)$  as for  $f(\alpha)$  shown by the dashed line which is similar to  $f(\alpha)$  in the localized phase of RRG [6]. (b) the triangular spectrum at the localization transition point  $\gamma = 2$ . It is identical to the one at  $W = W_{AT}$  on RRG; (c) the spectrum with the gap  $\alpha_{\min} = 2 - \gamma$  for the intermediate phase  $1 < \gamma < 2$ . It obeys the symmetry  $f(1+x) = f(1-x) + x$ ; (d) the degenerate spectrum for the ergodic phase at  $\gamma < 1$ . The ergodic transition at  $\gamma = 1$  corresponds to the collapse of  $\alpha_{\max} - \alpha_{\min} = 2(1 - \gamma)$ .

One can also introduce a singular  $f(\alpha)$  for  $\gamma > 2$  (see Fig. 2(a)). Its regular part is given by the same linear function Eq. (15) which, however, is valid down to  $\alpha = +0$ . At  $\alpha = 0$  there is a singular peak in  $f(\alpha)$  which summit corresponds to  $f(0) = 0$ . This singular  $f(\alpha)$  is not a limit of any *convex* function. However, one may easily see that all the moments  $N \langle |\psi|^2 q \rangle \sim N^{-\tau(q)}$  have the same exponents  $\tau(q)$  as for the “convex”  $f(\alpha)$  shown by the dashed line in Fig. 2 (a):  $f(\alpha) = \alpha/\gamma$  for  $0 < \alpha < \gamma$  and  $f(\alpha) = -\infty$  otherwise. Such a triangular  $f(\alpha)$  with the slope smaller than  $1/2$  is known in the localized phase on RRG [6].

From Fig. 2(c) it is obvious that the transition to the ergodic phase must occur at  $\gamma = 1$ . Indeed, at  $\gamma = 1$   $\alpha_{\min} = 2 - \gamma$  and  $\alpha_{\max} = \gamma$  collapse in one point  $\alpha = 1$  (Fig. 2(d)) corresponding to  $|\psi|^2 \sim 1/N$ . This is exactly the condition for the ergodic normalized wave function which “occupies” a finite fraction of the volume  $N$ .

*Numerical results*— In order to check the existence of the intermediate phase for  $1 < \gamma < 2$  we computed the average  $\langle x \ln x \rangle$  which is directly related with the Shannon entropy and the dimension  $D_1$  of the support set of fractal wave functions [14]. The results are shown in Fig. 3 where  $N$  spans from  $2^8$  up to  $2^{15}$ . The corresponding values of  $D_1$  extracted from the linear in  $\ln N$  fit are shown in the inset of Fig. 3 which are consistent with the transitions at  $\gamma = 2$  and  $\gamma = 1$ . The deviation from the expected  $D_1(\gamma)$  shown by a dashed line in the inset of Fig. 3 is a finite-size effect [10]. We also introduced the  $1/N$  corrections to the fit which magnitude  $C_{1/N}$  is a measure of the global curvature of the  $\langle x \ln x \rangle$  vs.  $\ln N$  dependence. Remarkably,  $C_{1/N}$  changes sign at  $\gamma \approx 1$

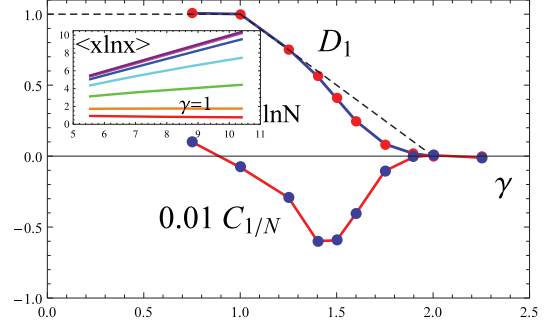


FIG. 3: (Color online) The support set dimension  $D_1(\gamma)$  and the global curvature  $C_{1/N}(\gamma)$  extracted from the fit  $\langle x \ln x \rangle = (1 - D_1) \ln N + C_0 + C_{1/N} N^{-1}$  vs.  $\gamma$ . The dashed line is the prediction for  $D_1$  based on  $f(\alpha)$  from Fig. 2; (inset) Shannon entropy of the RP model  $\langle x \ln x \rangle$  vs.  $\ln N$  for  $\gamma$  from 0.75 (bottom) to 2.25 (top) with steps 0.25; The global curvature  $C_{1/N}$  changes sign at the expected ergodic transition point  $\gamma \approx 1$ .

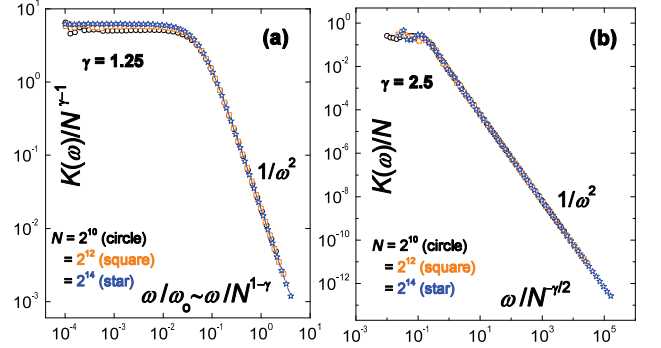


FIG. 4: (Color online) The overlap correlation function  $K(\omega) = N \sum_r \langle |\psi_E(r)|^2 |\psi_{E+\omega}(r)|^2 \rangle$ . (a) For  $1 < \gamma < 2$  the functions  $K(\omega) N^{1-\gamma}$  for different  $N$  collapse into the same curve in the coordinates  $\omega/\omega_o \propto \omega/N^{1-\gamma}$  (see also insert to Fig. 1). (b) For  $\gamma \geq 2$  the collapse occurs in the coordinates  $\omega/N^{-\gamma/2}$ . Thus at a fixed  $\omega$  and  $N \rightarrow \infty$  the function  $K(\omega) \rightarrow 0$  for  $\gamma > 1$ . This signals on the “repulsion of wave functions” at all energy separations  $\omega$  in the thermodynamic limit at  $\gamma > 1$ . For  $\gamma < 1$  a plateau  $K(\omega) \approx 1$  emerges which survives the thermodynamic limit. Such a plateau is a signature of an ergodic state [13].

and is very small for  $\gamma > 2$ . We believe that the changing of sign of  $C_{1/N}$  is a convenient way to identify the ergodic transition point. Finally, we computed the overlap of different wave functions. In Fig. 4 we demonstrate that for  $1 < \gamma < 2$  the onset of plateau is at  $\omega \sim \omega_o \propto N^{1-\gamma}$  while for  $\gamma > 2$  it occurs at  $\omega \propto N^{-\gamma/2}$ , in both cases the plateau moves to infinitely small  $\omega$  in the thermodynamic limit. In contrast, for  $\gamma < 1$  the onset of plateau occurs at  $\omega = E_0 \sim O(N^0)$  (which may exceed  $D \sim 1$ ). The emergence of such a plateau that survives the limit  $N \rightarrow \infty$  is a signature of the ergodic state [10, 13].

Surprisingly, the overlap function  $K(\omega) \rightarrow 0$  at any fixed  $\omega$  and  $\gamma > 1$  as  $N \rightarrow \infty$ . This new phenomenon

of “repulsion of wave functions” [15] is in our opinion typical for the AL on lattices with hierarchical structure.

In conclusion, we suggested a RM model in which the extended and non-ergodic phase exists in the finite range of parameters and is separated from the localized and extended ergodic phases by the two transition points. We presented both rigorous treatment of levels statistics in this model and perturbative arguments which unambiguously show the existence of two transition points. The results are supported by direct diagonalization of random matrices with sizes up to  $2^{15} = 32768$ .

*Acknowledgement* We are grateful to B. L. Altshuler, E. Bogomolny, L. B. Ioffe and J. P. Pekola for stimulating discussions. I.M.K acknowledges the support of the European Union Seventh Framework Programme IN-FERNOS (FP7/2007 - 2013) under grant agreement no. 308850 and of Academy of Finland (Project Nos. 284594, 272218). V.E.K. acknowledges the hospitality of Aalto University and at LPTMS of University of Paris Sud at Orsay and support under the CNRS grant ANR-11-IDEX-0003-02 Labex PALM, project MultiScreenGlass.

- [3] R. Abou-Chakra, P. W. Anderson and D. J. Thouless, *J. Phys. C: Solid State Physics*, **6**, 1734 (1993).
- [4] Y. V. Fyodorov and A. D. Mirlin, *Phys. Rev. Lett.* **67**, 2049 (1991); *Nucl. Phys. B* **336**, 507 (1991); *Phys. Rev. B* **56** 13393 (1997).
- [5] G. Birol, A. Ribeiro-Texiera, M. Tarzia, arXiv:1211.7334
- [6] A. De Luca, B. L. Altshuler, V. E. Kravtsov and A. Scardicchio, *Phys. Rev. Lett.* **113** 046806 (2014).
- [7] E. Targuini, G. Birol, M. Tarzia, arXiv:1507.00296
- [8] I. Oren, A. Godel and U. Smilansky *J. Phys. A: Math. Theor.* **42** 415101 (2009); I. Oren and U. Smilansky *J. Phys. A: Math. Theor.* **43** 225205 (2010).
- [9] H. Kunz and B. Shapiro, *Phys. Rev. E* **58**, 400 (1998).
- [10] see Supplementary Material for details.
- [11] F. Evers and A. D. Mirlin, *Rev. Mod. Phys.* **80**, 1355 (2008).
- [12] A. D. Mirlin, Y. V. Fyodorov, A. Mildenberger, and F. Evers, *Phys. Rev. Lett.* **97**, 046803 (2006).
- [13] E. Cuevas and V. E. Kravtsov, *Phys. Rev. B* **76**, 235119 (2007).
- [14] A. De Luca, A. Scardicchio, V. E. Kravtsov and B. L. Altshuler, arXiv:1401.0019.
- [15] This phenomenon was also observed in Ref. [13] for the Power-Law Banded Random Matrices and for the 3D Anderson model but only for large  $\omega > E_0 \sim D$ . For  $\omega < E_0$  there is an enhancement of overlap in these models.
- [16] J. T. Chalker, *Physica A* **167**, 253 (1990); J. T. Chalker, G. J. Daniell, *Phys. Rev. Lett.* **61**, 593 (1988).
- [17] V. E. Kravtsov, K. A. Muttalib, *Phys. Rev. Lett.* **79**, 1913 (1997).
- [18] A. D. Mirlin, Y. V. Fyodorov, F. M. Dittes, J. Quezada, T. H. Seligman, *Phys. Rev. E* **54**, 3221 (1996).

\* Electronic address: ivan.khaymovich@aalto.fi

- [1] D. M. Basko, I. L. Aleiner and B. L. Altshuler, *Annals of Physics* **321**, 1126 (2006).
- [2] V. Oganesyan, D. A. Huse, *Phys. Rev. B* **75**, 155111 (2007).

## Supplementary material

In this supplementary material we provide more details and results related to several points discussed in the main text.

### The spectral form-factor.

Eq. (2) of the paper can be cast as follows  $C(t, t') = e^{-\sigma(t^2+t'^2)/2} (K_1(t, t') + K_2(t, t'))$ , where:

$$K_1(t, t') = \frac{1}{N\tau\tau'} \oint_{\Gamma_R} \frac{dz}{2\pi i} \oint_{\Gamma_R} \frac{dz'}{2\pi i} e^{i(tz+t'z')} (g(z, z')^N - \rho(z)^N \rho(z')^N) , \quad (16)$$

$$K_2(t, t') = \frac{1}{N} \oint_{\Gamma_R} \frac{dz}{2\pi i} \oint_{\Gamma_R} \frac{dz'}{2\pi i} e^{i(tz+t'z')} \frac{g(z, z')^N}{(z' - z - \tau)(z' - z + \tau')} . \quad (17)$$

The definitions of the functions  $g(z, z')$  and  $\rho(z)$  are presented in the text of the paper.

Performing the re-scaling Eqs. (4, 6) of the paper and changing the variables  $y \rightarrow (q - q')y$  we arrive at:

$$K_1(t, t') = \sum_q \int \frac{p(x)dx}{a} e^{ixT - 2\pi\lambda^2 sqp(x)} \int \frac{dy}{2\pi} e^{ib(y - i\epsilon)} \left( e^{-\frac{ia}{y - i\epsilon}} - 1 \right) , \quad (18)$$

$$K_2(t, t') = \sum_q \int \frac{dx}{2\pi} e^{ixT - 2\pi\lambda^2 sqp(x)} \int \frac{dy}{4\pi} e^{ib(y - i\epsilon)} \frac{e^{-\frac{ia}{y - i\epsilon}}}{(y - i\epsilon + isq\lambda^2/2)^2} - \sum_q \int \frac{dx}{2\pi} e^{ixT} \int \frac{dy}{4\pi} e^{iby} \frac{1}{(y + isq\lambda^2/2)^2}, \quad (19)$$

where  $p(x)$  is the diagonal disorder distribution coinciding with the density of states for  $\gamma = 1$  [9] and the limit  $N \rightarrow \infty$  is taken everywhere, except in the exponents  $e^{i(tz+t'z')} \rightarrow e^{iN^{\gamma-2}sq(y-i\epsilon)}$ , the summation over  $q'$  is taken, and:

$$a = \pi\lambda^4 s^2 p(x), \quad b = 2sqN^{\gamma-2}. \quad (20)$$

The exponents determine the allowed contour deformations. Deforming the contour so that the exponents are small at  $|y| \rightarrow 0$  we observe that both  $K_1(t, t')$  and  $K_2(t, t')$  are identically zero for  $sq < 0$ . Thus the summation over  $q$  can be dropped with  $s$  being replaced by  $|s|$ . One can also express the integrals over  $y$  in terms of the Bessel functions, deforming the contour so that it encompasses the origin along the infinitesimal circle. The final result for  $C(t, t') = 2\pi\delta(t + t') [S(u = s/p(0), \Lambda = \lambda p(0), N, \gamma) - 1]$  reads:

$$\begin{aligned} S(u, \Lambda, N, \gamma) &= 1 + e^{-2\pi\Lambda^2 u} \frac{2e^{-\Lambda^2 u^2 N^{\gamma-2}}}{\sqrt{8\pi N^{\gamma-2} \Lambda^4 u^3}} I_1(\sqrt{8\pi N^{\gamma-2} \Lambda^4 u^3}) \\ &\quad - \frac{1}{4\pi} \sqrt{8\pi\Lambda^4 u^5} N^{(3\gamma-6)/2} e^{-2\pi\Lambda^2 u} e^{-\Lambda^2 u^2 N^{\gamma-2}} \int_0^\infty \frac{x dx}{\sqrt{x+1}} I_1(\sqrt{8\pi N^{\gamma-2} \Lambda^4 u^3 (x+1)}) e^{-x u^2 \Lambda^2 N^{\gamma-2}}, \end{aligned} \quad (21)$$

where  $I_1(x)$  is the modified Bessel function and  $\Lambda = \lambda p(0)$ . Eq. (21) is valid for  $\gamma > 1$ .

The unfolded spectrum form factor is given by:

$$R(t \equiv (t - t')\delta) = S(tN^{2-\gamma}, \Lambda, N, \gamma), \quad (22)$$

where  $\delta$  is the mean level spacing.

For  $\gamma > 2$  one can see that  $R(t)$  tends to the Poisson limit  $R(t) = 1$  as  $N \rightarrow \infty$ .

For  $1 < \gamma < 2$  and any  $t > 0$  it evolves towards the GUE form factor:

$$R_{GUE}(t) = \begin{cases} t, & 0 \leq t < 2\pi \\ 1, & t \geq 2\pi \end{cases}, \quad (23)$$

as  $N \rightarrow \infty$ .

However, in contrast to  $R_{GUE}(t)$  the function  $R(t)$  has a jump at  $t = 0$ :

$$R(t = 0) = 1. \quad (24)$$

On the other hand, the function  $S(u \equiv (t - t')\omega_o, \Lambda, N, \gamma) = R(uN^{\gamma-2})$  at  $1 < \gamma < 2$  has a finite non-singular limit as  $N \rightarrow \infty$ :

$$\lim_{N \rightarrow \infty} R(uN^{\gamma-2}) = e^{-2\pi\Lambda^2 u}, \quad (25)$$

while for the true GUE form-factor this limit is zero:

$$\lim_{N \rightarrow \infty} R_{GUE}(uN^{\gamma-2}) = 0. \quad (26)$$

The limit Eq. (25) and the new emergent scale

$$\omega_o = \delta N^{2-\gamma} \sim N^{1-\gamma}. \quad (27)$$

is a hallmark of the intermediate extended and non-ergodic state for  $1 < \gamma < 2$ .

### Moments of $|\psi|^2$ .

Here we discuss the moments

$$I_q = \left\langle \sum_r |\psi(r)|^{2q} \right\rangle = N \langle |\psi|^{2q} \rangle \propto N^{-\tau(q)}. \quad (28)$$

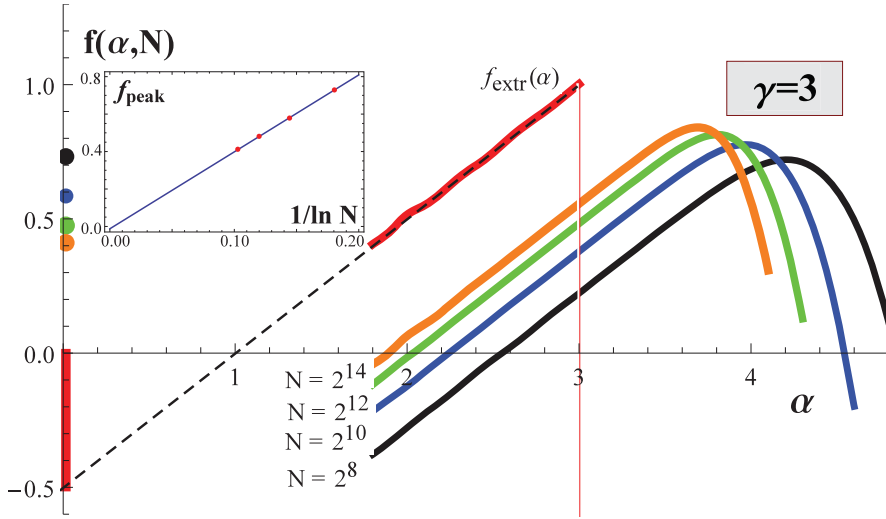


FIG. 5: (Color online) Spectrum of fractal dimension for  $\gamma = 3$ . The linear part of the extrapolated  $f(\alpha)$  (solid red line) is exactly as expected  $f(\alpha)$  (black dashed line). The curves for  $f(\alpha, N)$  for different  $N$  are shown by black, blue, green and orange lines. The top of the singular peak at  $\alpha = 0$  shown by the points of the corresponding color is close to zero as expected (see inset); (inset) the  $1/\ln N$  extrapolation of the singular peak value  $f_{peak} = f(0, N)$ .

We start by considering the localized phase  $\gamma > 2$  where the moments with  $q \geq 1$  are dominated by the singular term  $N^{-1}\delta(x - N)$  in the distribution function. One can easily see that all such moments are  $N$ -independent, which corresponds to  $\tau(q) = 0$ . Using this equality and given that  $\tau(q)$  and  $f(\alpha)$  are related by the Legendre transform [11]:

$$\tau(q) = q\alpha_q - f(\alpha_q), \quad f'(\alpha_q) = q, \quad (29)$$

and that the singular peak is located at  $\alpha = 0$ , one immediately obtains that the top of the peak corresponds to  $f(0) = 0$ . Considering also  $q < 1$  and using the Legendre transform Eq.(29) we obtain from  $f(\alpha)$  of Fig.2 of the paper:

$$\tau(q) = \begin{cases} \gamma q - 1, & q < 1/\gamma, \\ 0, & q > 1/\gamma, \end{cases} \quad (\gamma > 2). \quad (30)$$

By the nature of the Legendre transform the tangential to  $f(\alpha)$  with any slope  $q$  is the same for the singular and "non-convex"  $f(\alpha)$  shown by the red solid line in Fig.2(a) of the paper and for the "convex"  $f(\alpha)$  shown by the blue dashed line. Thus for both types of  $f(\alpha)$  shown in Fig.2(a) of the paper  $\tau(q)$  is given by Eq.(30).

For  $1 < \gamma < 2$  Eq.(29) gives:

$$\tau(q) = \begin{cases} \gamma q - 1, & q < 1/2, \\ (2 - \gamma)(q - 1), & q > 1/2, \end{cases} \quad (1 < \gamma < 2). \quad (31)$$

#### Numerical extrapolation of the spectrum of fractal dimensions.

We computed the distribution function  $P(x)$  of the normalized amplitude  $x = N|\psi|^2$  and extracted the spectrum of fractal dimensions  $f(\alpha, N) = \ln(N P_{env}(\ln N(1 - \alpha))) / \ln N$ , using the approach of Ref.[6]. In order to eliminate the effect of zeros of wave functions  $\psi$  which dominate the distribution function  $P(x)$  at small  $x < x_{min} \sim N^{1-\gamma}$  and extract the distribution function of a smooth envelope of  $|\psi|^2$  we represent  $\psi = \psi_{env} \times \eta$ , where  $\eta$  is the GOE random oscillations with the unit average square which are supposed to be statistically independent of  $\psi_{env}$ . Then the distribution of  $\ln x$  is a convolution of the distribution  $P_{env}(y)$  of  $y = \ln x_{env} = \ln(N\psi_{env}^2)$  and the known GOE distribution of  $\ln \eta^2$ . Making a numerical de-convolution one obtains the distribution  $P_{env}(y)$  in which the effect of zeros of  $\eta(r_o)$  is eliminated. Such a "rectified" distribution function decreases much faster at small  $x_{env} < x_{min}$  than the distribution  $P(\ln x)$ . This "rectification procedure" results in a sharp cut-off of  $f(\alpha, N)$  at large  $\alpha$ . Then the so obtained  $f(\alpha, N)$  is extrapolated to  $N = \infty$  using the ansatz [6]  $f(\alpha, N) = f(\alpha) + c(\alpha)/\ln N$ .

The results for the localized case  $\gamma = 3$  and  $N = 2^8 \dots 2^{14}$  are shown in Fig. 5. One can see that  $f(\alpha)$  rectified and extrapolated as explained above has a linear in  $\alpha$  part which exactly coincides with the prediction of the paper (see

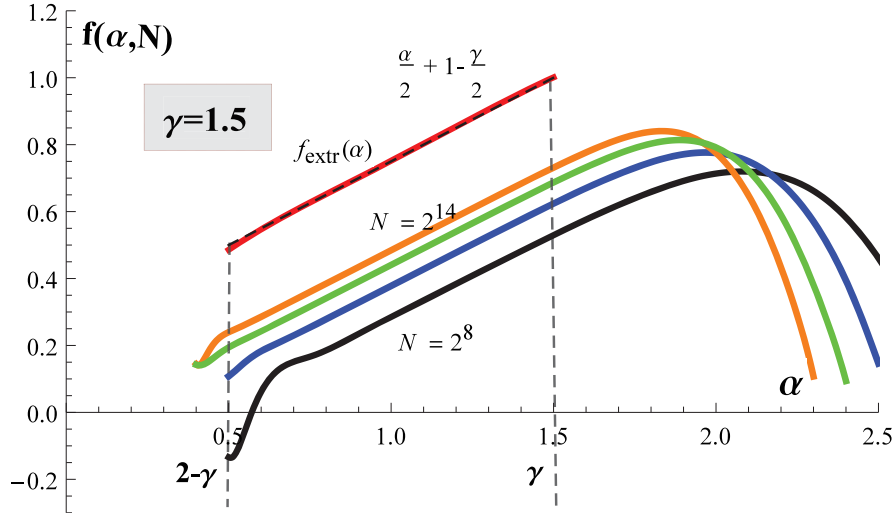


FIG. 6: (Color online) Spectrum of fractal dimension for  $\gamma = 1.5$ . Extrapolated  $f(\alpha)$  is shown by the red line. Expected  $f(\alpha)$  is shown by a dashed line. The curves for  $f(\alpha, N)$  for different  $N$  are shown by blue, green, yellow and orange lines.

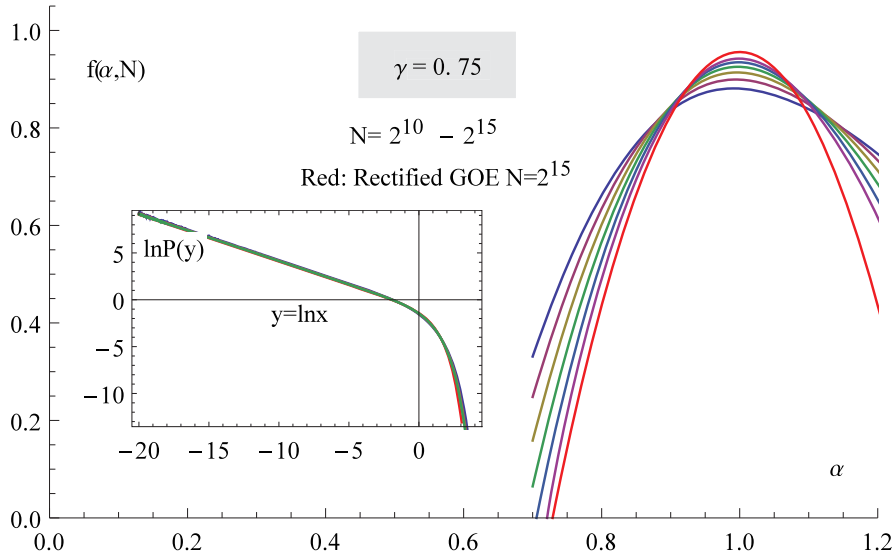


FIG. 7: (Color online) Finite- $N$  spectrum of fractal dimensions  $f(\alpha, N)$  for  $\gamma = 0.75$  and  $N = 2^{10} - 2^{15}$  obtained by the rectification procedure of Ref. [6]. For comparison we also present  $f(\alpha, N)$  (shown by a red line) for the Porter-Thomas distribution of wave function amplitudes in the GOE obtained by the same procedure at  $N = 2^{15}$ . It almost coincides with the (violet) curve for  $f(\alpha, N)$  computed at the same  $N = 2^{15}$  for our model with  $\gamma = 0.75$ . In the insert:  $\ln P(x)$  vs  $\ln x$  for the same  $\gamma = 0.75$  and system sizes as in the main plot. The corresponding curve for GOE is shown in red.

Fig. 2 of the paper). Moreover, the singular peak predicted for  $\gamma > 2$  in the paper is observed and its top value tends to zero as  $N \rightarrow \infty$  (see inset in Fig. 5). In Fig. 6 we present the extrapolated  $f(\alpha)$  for  $\gamma = 1.5$ . Again, the linear part of  $f(\alpha)$  coincides with the expectation shown in Fig. 2 of the paper. Finally, we present the results for  $f(\alpha, N)$  for  $\gamma = 0.75 < 1$ . One can see that the distribution function  $P(x)$  is weakly  $N$ -dependent and is almost indistinguishable on the logarithmic scale from the Gaussian Orthogonal Ensemble (GOE) distribution function. The function  $f(\alpha, N)$  is more sensitive to  $N$  but also in this case there is a minor difference from the corresponding GOE result.

#### Absence of Chalker's scaling and repulsion of wave functions.

Conventional multifractal correlations imply not only a power-law scaling of the moments of  $|\psi_n(r_o)|^2$  with the system size  $N$  but also a specific power-law two- and multi- point correlations. In particular, the overlap correlation

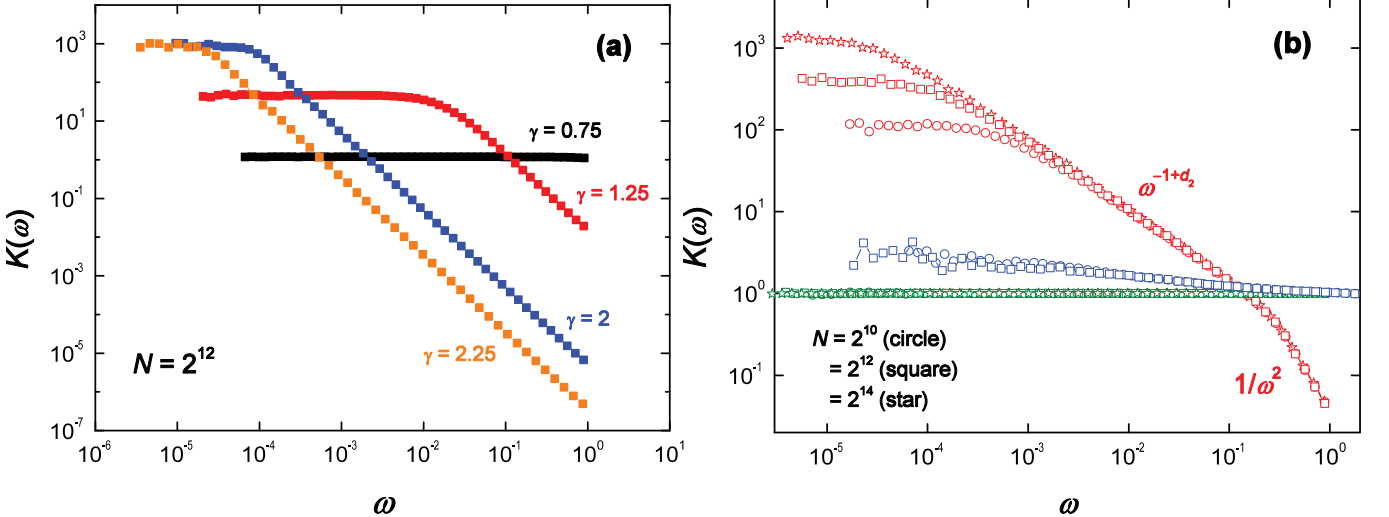


FIG. 8: (Color online) Overlap correlation function Eq. (32): (a) for the Rosenzweig-Porter model at different  $\gamma$  at  $N = 2^{12}$ ; (b) for the PLBRM model (red symbols), GOE (green symbols) and banded random matrix model (blue symbols). There are three regions with different behavior for the PLBRM: the plateau, the Chalker's scaling with the non-trivial exponent  $\omega^{-1+D_2}$ , the fast decay  $\sim \omega^{-2}$ . Only two of these three regimes are present on the plot (a): the Chalker's scaling is absent. The GOE behavior  $K(\omega) = \text{const}$  is identical to the one for RP model at  $\gamma = 0.75$ . Note that the behavior in the localized region  $\gamma > 2$  of the RP model is qualitatively different from that of the quasi-one dimensional localization in the banded random matrices: in the former case the repulsion of wave functions is present, while in the latter case positions of centers of localization are randomly distributed in space with almost no correlations.

function:

$$K(\omega) = N \sum_r |\psi_E(r)|^2 |\psi_{E+\omega}(r)|^2 \sim \left( \frac{E_0}{\omega} \right)^\mu, \quad \mu = (1 - D_2), \quad (32)$$

for  $\delta < \omega < E_0$  (with  $E_0 \sim O(1)$  being the onset of the anti-correlations) obeys the Chalker's scaling [13, 16, 17] in the energy domain. Eq. (32) holds exactly at the critical point of the 3D Anderson model and in certain random matrix ensembles, e.g. for the power law banded random matrices (PLBRM) [17, 18]. It implies an enhancement of correlations compared to the case of independently fluctuating wave function which would result in  $K(\omega) = 1$ . However, Eq. (32) is also approximately valid in the metallic phase of the 3D Anderson model close to the transition point [13] in the limited range of  $\delta_\xi < \omega < E_0$ , where  $\delta_\xi = (\rho N_c)^{-1}$  is the mean level spacing in the correlation volume  $N_c \sim \xi^3$ . For  $\omega < \delta_\xi$  the correlation function saturates developing a plateau, and for  $\omega > E_0$  it decreases fast as  $\omega^{-2}$  [13]. In the 3D Anderson model the plateau survives the thermodynamic limit  $N \rightarrow \infty$  and extends to larger  $\omega$  as one goes deeply into the metallic phase. It is thus a signature of the ergodic extended state. In the region  $\omega > E_0$ , the overlap correlation function is small, which signals on the “repulsion of wave functions” at large energy separations [13]. A similar phenomenon of eigenfunction repulsion for  $\omega > E_0$  was observed in the PLBRM with a small bandwidth  $b$  (see [13] or Fig. 8(b)).

We calculated  $K(\omega)$  in our model numerically. The result is presented in Fig. 4 of the paper and in Fig. 8(a) in the SM. Surprisingly, no Chalker's scaling and enhancement of correlations similar to Eq. (32) was observed. For  $1 < \gamma < 2$  the correlations are fast decreasing at  $\omega > E_0 \sim N^{1-\gamma}$ :

$$K(\omega) \sim \begin{cases} N^{1-\gamma} \omega^{-2}, & \omega > E_0 \sim N^{1-\gamma} \\ N^{\gamma-1}, & \omega < E_0 \end{cases}, \quad (1 < \gamma < 2) \quad (33)$$

like in the high-energy region  $\omega > E_0$  of the 3D Anderson and PLBRM models. The plateau is present only in a narrow interval of small  $\omega < E_0 \sim 1/N^{\gamma-1}$  which shrinks to zero in the thermodynamic limit. Note that in this case the onset of the anti-correlations  $\omega < E_0 \sim \omega_o$  scales as the parameter  $\omega_o = \delta N^{2-\gamma}$  which enters the dimensionless variable  $u = (t - t')\omega_o$  in the unfolded spectral form-factor  $S(u)$  in the level statistics (shown in the inset of Fig. 1 in the main text).

Qualitatively similar (but quantitatively different) behavior is observed in the localized phase  $\gamma > 2$ :

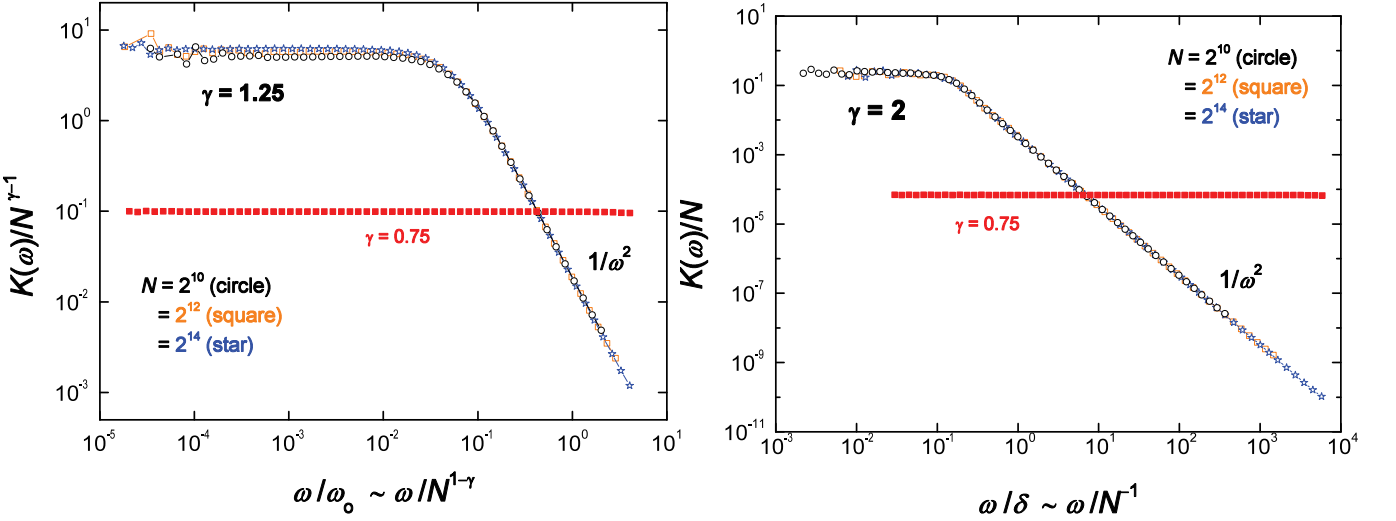


FIG. 9: (Color online) Collapse of data for  $K(\omega)$  at  $\gamma = 1.25$  and  $\gamma = 2.00$  in the coordinates  $X = \omega/N^{1-\gamma}$ ,  $Y = K(\omega)N^{1-\gamma}$ . For comparison the data for  $\gamma = 0.75$  and  $N = 2^{12}$  are shown in the same coordinates.

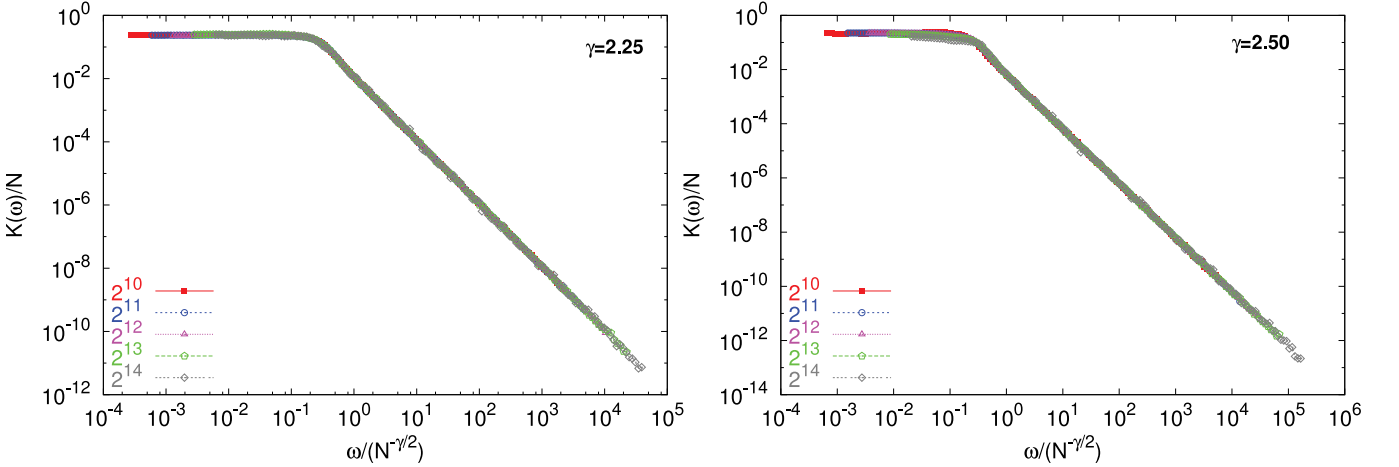


FIG. 10: (Color online) Collapse of data for  $K(\omega)$  at  $\gamma = 2.25$  and  $\gamma = 2.50$  in the coordinates  $X = \omega/N^{-\gamma/2}$ ,  $Y = K(\omega)/N$ .

$$K(\omega) \sim \begin{cases} N^{1-\gamma} \omega^{-2}, & \omega > E_0 \sim N^{-\gamma/2} \\ N, & \omega < E_0 \end{cases}, \quad (\gamma > 2) \quad (34)$$

Surprisingly at  $\gamma > 1$  and a fixed  $\omega$  the overlap  $K(\omega)$  drops below the independent wave function limit  $K(\omega) = 1$ . Thus in  $N \rightarrow \infty$  limit of our model for  $\gamma > 1$  the repulsion of wave functions happens at all energy scales.

For  $\gamma < 1$  the plateau  $\sim 1$  in  $K(\omega)$  extends to almost the entire spectral bandwidth  $D$  (see Fig. 8(a)), as  $E_0 \sim O(1)$  and may even exceed the spectral bandwidth. The emergence at  $\gamma = 1$  of a plateau that survives the thermodynamic limit and occupies a finite fraction of (or all of) the spectral bandwidth is a very clear signature of the ergodic transition at  $\gamma = 1$ .

Eqs. (33, 34) were checked by a collapse of the data points for a fixed  $\gamma$  but different  $N = 2^{10} - 2^{14}$ . The results are shown in Fig. 9 and Fig. 10. As  $\gamma$  approaches the Anderson transition point  $\gamma = 2$  deviations from Eq. (33) emerge. For  $1 < \gamma < 2$  the best collapse was found to occur in the coordinates  $X = \omega N^{\Delta_X(\gamma)}$ ,  $Y = K(\omega)N^{\Delta_Y(\gamma)}$ , where:

$$\Delta_X(\gamma) = \gamma - 1 + d, \quad \Delta_Y(\gamma) = \gamma - 1 - 2d. \quad (35)$$

The correction  $d(\gamma)$  is most probably due to the finite-size  $N$  that could be comparable with the correlation volume near the Anderson transition point  $\gamma = 2$ . The dependence  $1 + \Delta_X(\gamma)$  vs.  $\gamma$  is plotted in Fig. 12b. It has an apparent analogy with the dependence  $D_1(\gamma)$  of the support set dimension in Fig. 12a.

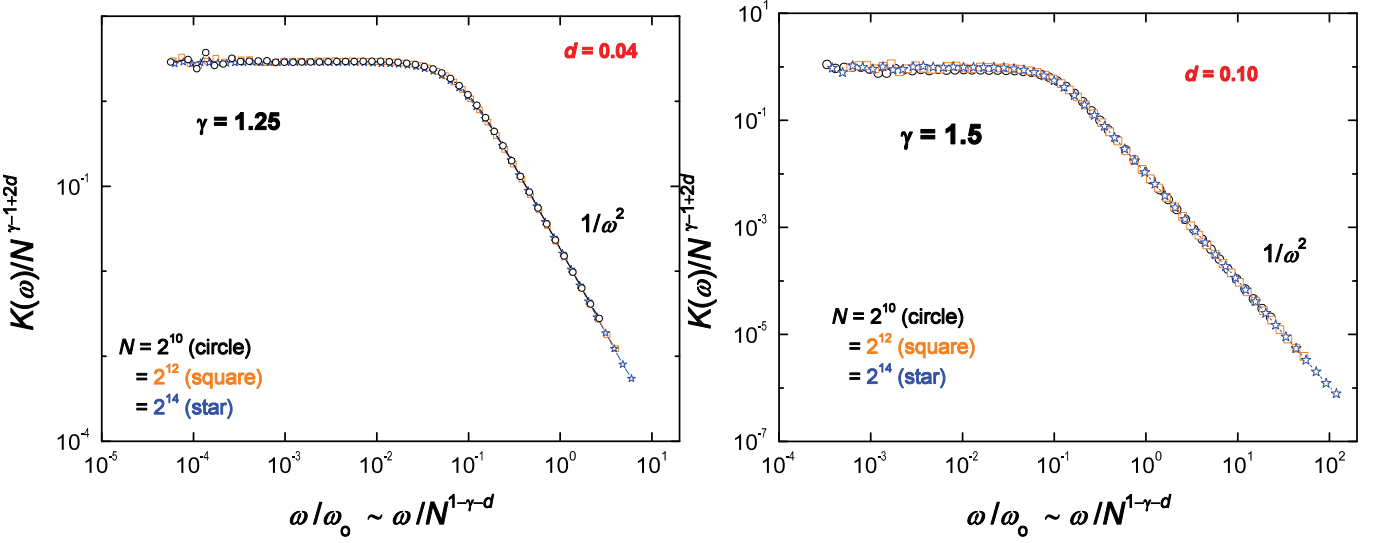


FIG. 11: (Color online) Collapse of data for  $K(\omega)$  at  $\gamma = 1.25$  and  $\gamma = 1.50$  in the coordinates  $X = \omega/N^{1-\gamma-d}$ ,  $Y = K(\omega)N^{1-\gamma-2d}$ . The corrections  $d = 0.04$  and  $d = 0.10$  are obtained from the best collapse.

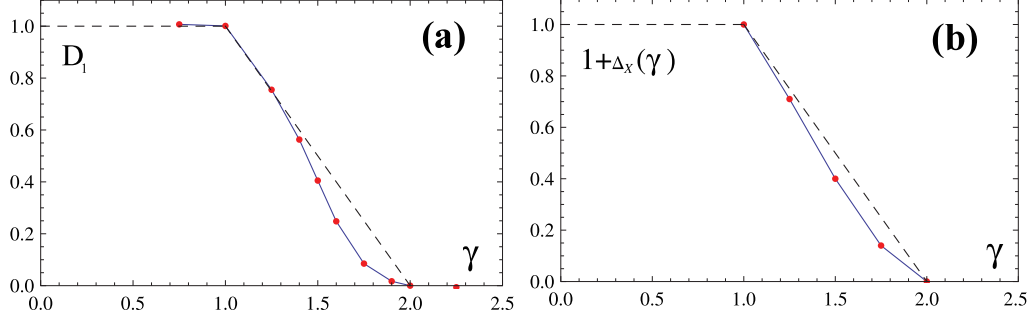


FIG. 12: (Color online) (a) The support set dimension  $D_1$  vs.  $\gamma$ . (b) The scaling exponent  $\Delta_X(\gamma)$  vs.  $\gamma$ . In both cases the finite-size effects make  $D_1$  and  $1 + \Delta_X$  closer to its value at  $\gamma = 2$  than expected (dashed line).

#### Support set dimension and the curvature.

We computed numerically the moment  $\langle x \ln x \rangle$ , where  $x = N |\psi|^2$ , which in a pure multifractal state should behave as:

$$\langle x \ln x \rangle = (1 - D_1) \ln N + \text{const.}, \quad (N \rightarrow \infty), \quad (36)$$

where  $D_1$  is a dimension of the wavefunction support set. In an ergodic phase  $D_1 = 1$ , while in the localized phase  $D_1 = 0$ . In the intermediate multifractal state  $0 < D_1 < 1$ . The support set dimension [14] may be expressed through the solution  $\alpha = \alpha_1$  of the equation (with  $f(\alpha)$  being a spectrum of fractal dimensions):

$$f'(\alpha) = 1, \quad (37)$$

i.e.  $D_1 = \alpha_1$  is a point  $\alpha = \alpha_1$  where the line with the slope 1 is tangential to  $f(\alpha)$ . One can immediately calculate  $D_1$  as a function of  $\gamma$  using Fig. 2 of the paper:

$$D_1 = \begin{cases} 1, & (\gamma < 1) \\ 2 - \gamma, & (1 < \gamma < 2) \\ 0, & (\gamma > 2) \end{cases} \quad (38)$$

The dependence of the moments  $I_1 = \langle x \ln x \rangle$  vs.  $\ln N$  is shown in Fig. 14 of the paper for  $N = 2^8, 2^9, \dots, 2^{15}$ . By fitting to Eq. (36) one can find  $D_1$  and compare it with the expected result Eq. (38). The comparison is shown in

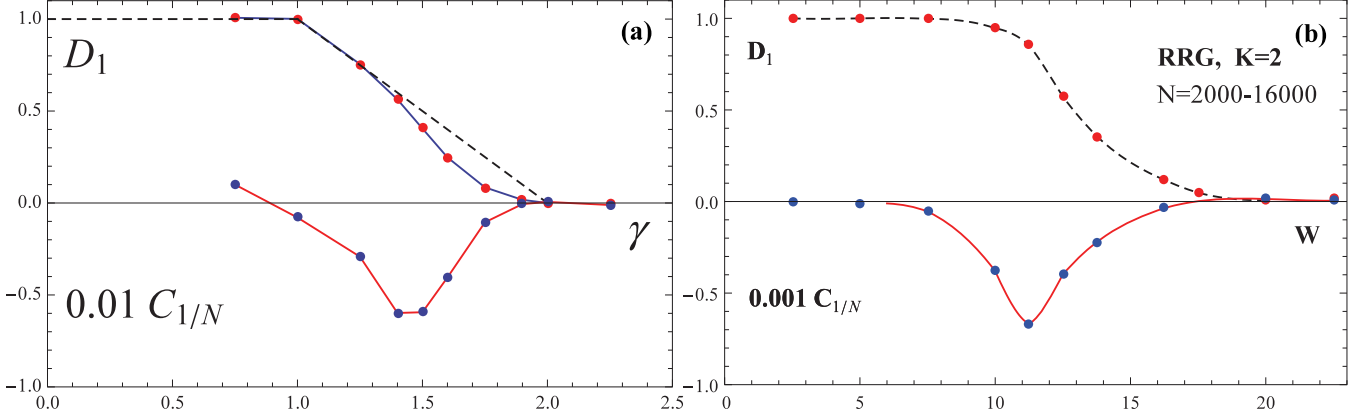


FIG. 13: (Color online) The apparent support set dimension  $D_1$  and the global curvature  $C_{1/N}$  (a) vs.  $\gamma$  for the Rosenzweig-Porter model; (b) vs. the strength of disorder  $W$  for the RRG with the branching number  $K = 2$ . The dashed line in (a) shows the result of Eq. (38). The curvature changes sign close to expected ergodic transition. In (b) the change of sign (poorly visible) of the curvature occurs at the Anderson localization transition at  $W \approx 18$ . There is no change of sign for  $W < W_{AT}$  down to  $W = 2.5$  though the curvature is very small and  $D_1$  is very close to 1 for  $W < 7.5$ .

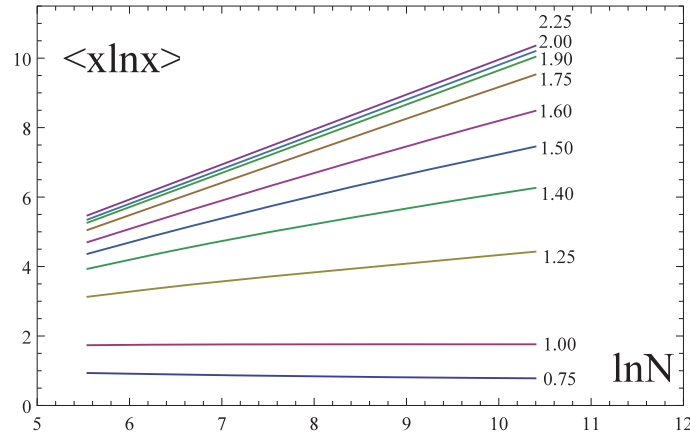


FIG. 14: (Color online) Shannon entropy of the RP model  $\langle x \ln x \rangle$  vs.  $\ln N$  for different  $\gamma = 0.75, 1.00, 1.25, 1.40, 1.50, 1.60, 1.75, 1.90, 2.00, 2.25$  from bottom to top.

Fig. 13(a). One can see that the apparent  $D_1$  extracted from limited sizes  $N = 2^8 - 2^{15}$  deviates from the prediction Eq. (38) as  $\gamma$  approaches the Anderson transition point  $\gamma = 2$ . We believe that this is a finite-size effect related to the correlation volume  $N_c$  that diverges exponentially at the transition. Clearly, for  $N < N_c$ , one should see the properties of the critical point where  $D_1 = 0$ . That is why the apparent  $D_1$  is smaller as the prediction in the vicinity of  $\gamma = 2$ . At the same time, Eq. (38) describes very well the data points for  $D_1$  close to  $\gamma = 1$ . This probably means that the ergodic transition is not associated with an exponentially divergent correlation length.

One can quantify the deviations from the linear behavior Eq. (36) by introducing the  $1/N$  correction which has a finite curvature in the  $\ln N$  variable. In reality, the finite-size scaling exponents are not known for this model, and the true corrections could be very different from  $1/N$ . However, coefficient  $C_{1/N}$  in the simple fit:

$$\langle x \ln x \rangle = (1 - D_1) \ln N + c_0 + C_{1/N} N^{-1} \quad (39)$$

gives an idea about the “global curvature” of the dependence  $\langle x \ln x \rangle$  vs.  $\ln N$ . The dependence of this coefficient on  $\gamma$  is shown in Fig. 13(a). It has a characteristic peak shape. For  $\gamma$  in the vicinity of 1 the finite-size effects are small at our system sizes, and the global curvature is small too. Close to the point  $\gamma = 2$  our system sizes are far too small to deviate from the critical behavior at the transition point. In this case the global curvature is small too. The absolute value of the global curvature reaches its maximum where  $\ln N \sim \ln N_c$ .

An important observation is that the “global curvature” changes sign at the ergodic transition. This observation may be used to locate the transition point in finite-size calculations.

In addition to the global curvature one may also introduce a “local curvatures” as follows:

$$\kappa_< = \frac{(I_1[[1]] + I_1[[3]] - 2I_1[[2]])/\ln^2 2}{(1 + (I_1[[1]] - I_1[[3]])^2/4\ln^2 2)^{3/2}}, \quad \kappa_> = \frac{(I_1[[1]] + I_1[[3]] - 2I_1[[2]])/\ln^2 2}{(1 + (I_1[[1]] - I_1[[3]])^2/4\ln^2 2)^{3/2}}, \quad (40)$$

where  $I_1[[i]]$  is a moment  $I_1$  for the  $i$ -th system size counted from the first one  $N = 2^8$ , while  $I_1[[[-i]]]$  is the moment  $I_1$  for the  $i$ -th system size counted from the last one  $N = 2^{15}$ . Eq. (40) is nothing but the discrete variant of the curvature:

$$\kappa = \frac{h''(x)}{(1 + [h'(x)]^2)^{3/2}} \quad (41)$$

of a curve given by a function  $h(x)$ .

In the table below we present  $\kappa_<$  and  $\kappa_>$  for different  $\gamma$ . One can see that the local, as well as the global curvature

TABLE I: Local curvatures  $\kappa_<$  and  $\kappa_>$ .

	$\kappa_< \times 10$	$\kappa_> \times 10$
$\gamma = 0.75$	+0.05	+0.05
$\gamma = 1.00$	-0.16	0.03
$\gamma = 1.25$	-0.42	-0.10
$\gamma = 1.40$	-0.40	-0.27
$\gamma = 1.60$	-0.13	-0.17
$\gamma = 1.75$	-0.03	-0.06
$\gamma = 2.00$	0.00	0.00
$\gamma = 2.25$	0.00	0.00

is negative for  $1 < \gamma < 2$ . It is positive and small for  $\gamma = 0.75 < 1$ . Thus it is likely, that the local curvature, too, changes sign close to the ergodic transition at  $\gamma = 1$ . The absolute value of  $\kappa$  decrease with increasing  $N$  in the vicinity of  $\gamma = 1$  (for  $\gamma = 1.25$  and  $\gamma = 1.40$ ), which signals about convergence. In contrast  $|\kappa|$  increase with increasing  $N$  in the vicinity of  $\gamma = 2$  (for  $\gamma = 1.6$  and  $\gamma = 1.75$ ) as the system size  $N$  approaches the correlation volume from below. For  $\gamma = 2.0$  and  $\gamma = 2.25$  the local curvature is very small and is inside the error bar.

#### Comparison with the RRG model.

The same analysis of the moments  $\langle x \ln x \rangle$  for the Random Regular Graph (RRG) leads to the results presented in Fig. 13(b). It is similar to Fig. 13(a) but the difference is that the global curvature  $C_{1/N}$  changes sign at the Anderson localization transition  $W \approx 18$ , and no other point of change of sign is detected down to very small disorder strength  $W$ .